Earth and Planetary Science Letters 415 (2015) 38–46

Contents lists available at ScienceDirect

Earth and Planetary Science Letters

www.elsevier.com/locate/epsl

Alteration of ocean crust provides a strong temperature dependent feedback on the geological carbon cycle and is a primary driver of the Sr-isotopic composition of seawater

Laurence A. Coogan *, Stan E. Dosso

School of Earth and Ocean Sciences, University of Victoria, Victoria, BC, Canada

ARTICLE INFO

Article history:
Received 2 September 2014
Received in revised form 11 January 2015
Accepted 23 January 2015
Available online 9 February 2015
Editor: G.M. Henderson

Keywords:
long-term carbon cycle
off-axis hydrothermal circulation
seawater composition
Sr-isotopes

ABSTRACT

On geological timescales there is a temperature dependent feedback that means that increased degassing of CO_2 into the atmosphere leads to increased CO_2 drawdown into rocks stabilizing Earth's climate. It is widely considered that this thermostat largely comes from continental chemical weathering. An alternative, or additional, feedback comes from dissolution of seafloor basalt in low-temperature (tens of °C), off-axis, hydrothermal systems. Carbonate minerals precipitated in these systems provide strong evidence that increased bottom water temperature (traced by their O-isotopic compositions) leads to increased basalt dissolution (traced by their Sr-isotopic compositions). Inversion of a simple probabilistic model of fluid–rock interaction allows us to determine the apparent activation energy of rock dissolution in these systems. The high value we find (92 ± 7 kJ mol^{-1}) indicates a strong temperature dependence of rock dissolution. Because deep-ocean temperature is sensitive to global climate, and the fluid temperature in the upper oceanic crust is strongly influenced by bottom water temperature, increased global temperature must lead to increased basalt dissolution. In turn, through the generation of alkalinity by rock dissolution, this leads to a negative feedback on planetary warming; i.e. off-axis, hydrothermal systems play an important role in the planetary thermostat. Changes in the extent of rock dissolution, due to changes in bottom water temperature, also lead to changes in the flux of unradiogenic Sr into the ocean. The decreased flux of unradiogenic Sr into the ocean due to the cooling of ocean bottom water over the last 35 Myr is sufficient to explain most of the increase in seawater $^{87}Sr/^{86}Sr$ over this time.

1. Introduction

The long-term carbon cycle is, to a first order, controlled by volcanic and metamorphic CO_2 degassing and the drawdown of CO_2 into carbonate minerals (Walker et al., 1981). The feedback processes that control the fine balance between degassing and drawdown are critical to maintaining a habitable planet (Berner and Caldeira, 1997) but are incompletely understood. The generally accepted mechanism for this planetary thermostat is that increased atmospheric CO_2 leads to increased surface temperature and precipitation and hence increased rates of CO_2 consumption via continental weathering (e.g., Walker et al., 1981; Berner et al., 1983; Berner, 2004 and references therein). This basic model has been developed to include many other factors such as: (i) changes in continental weatherability due to tectonic processes (e.g., Raymo and Ruddiman, 1992) and variations in vegetation (e.g., Pagani et al., 2009); and (ii) organic carbon cycling (e.g., France-Lanord and Derry, 1997). However, the basic premise of the model remains that continental chemical weathering is central to the long-term carbon cycle.

An alternative feedback mechanism that could control the long-term carbon cycle comes from the reaction of seawater with the oceanic crust in low-temperature, off-axis, hydrothermal systems (Francois and Walker, 1992; Brady and Gislason, 1997; Sleep and Zahnle, 2001; Gillis and Coogan, 2011; Coogan and Gillis, 2013). It has been argued that variations in deep-water pH are too small for changes in the deep ocean hydrogen ion concentration to provide a feedback on the long-term carbon cycle (Caldeira, 1995). However, variations in deep-water temperature (Brady and Gislason, 1997), perhaps combined with variations in seawater major element composition (Coogan and Gillis, 2013), provide viable feedback mechanisms. Off-axis hydrothermal systems circulate a volume of seawater equivalent to the entire ocean through the upper oceanic crust every few hundred thousand years (e.g., Johnson and Pruis, 2003). Fluid flows through the permeable upper crust (lavas) where it is heated by the cooling of the ocean lithosphere be-

* Corresponding author. Tel.: +1 250 472 4018.
E-mail address: lacoogan@uvic.ca (L.A. Coogan).

http://dx.doi.org/10.1016/j.epsl.2015.01.027
0012-821X/

fore discharging back out of this aquifer into the ocean (e.g., Fisher and Becker, 2000). Reactions within the crust generate the alkalinity required for carbonate mineral precipitation (Coogan and Gillis, 2013). Because reaction rates are temperature sensitive, the extent of fluid–rock reaction within the crust is expected to depend on the temperature of the water entering the crust (i.e. ocean bottom water), providing a temperature-dependent feedback on CO_2 consumption (Brady and Gislason, 1997). This model is supported by the observation of higher CO_2 contents in altered late Mesozoic upper oceanic crust than late Cenozoic upper oceanic crust (Gillis and Coogan, 2011).

Carbonate minerals are found in the lava section of the crust where they occur in veins, filling pore spaces and replacing igneous phases (e.g., Staudigel et al., 1981; Alt and Teagle, 1999; Coggon et al., 2004; Gillis and Coogan, 2011; Rausch et al., 2013). Bulk-rock CO_2 contents are controlled by the abundance of secondary carbonates. These range from ~0.5 to 4.0 wt% (Gillis and Coogan, 2011 and references therein) indicating a substantial C sink. Because deep seawater is not saturated with carbonate minerals, reactions in the crust are required to drive the precipitation of significant masses of carbonate minerals. It has been suggested that the carbonate mineral forming reactions involve Ca leaching from the rock charge balanced by Mg uptake into the rock (e.g., Berner, 2004). However, models of fluid–rock reaction show that neither leaching Ca from the crust charge balanced by exchange for Mg (i.e., without alkalinity generation), nor heating the hydrothermal fluid, can drive the precipitation of substantial amounts of carbonate. Instead carbonate mineral precipitation is largely driven by alkalinity generation (Spivack and Staudigel, 1994; Coogan and Gillis, 2013). The compositions of carbonate minerals thus provide information about the conditions within the crust during this alkalinity production.

Understanding past rates of chemical weathering of the continents, and paleo-hydrothermal chemical fluxes, is difficult. Perhaps the most widely used tracer of the relative rates of chemical dissolution of continental crust and mantle-derived (basaltic) material is the Sr-isotopic composition of seawater for which there is an exquisite paleo-record (e.g., Veizer et al., 1999). The simplest interpretation of variations in the Sr-isotopic composition of seawater is that an increase in $^{87}Sr/^{86}Sr$ indicates a relative increase in the flux of Sr from old continental material (high Rb/Sr). Conversely, a decrease in seawater $^{87}Sr/^{86}Sr$ indicates a relative increase in the flux of Sr from mantle-derived (or juvenile) material with low time-integrated Rb/Sr. The large increase in seawater $^{87}Sr/^{86}Sr$ over the last ~35 Myr is widely considered to largely reflect an increased flux of radiogenic Sr from rivers draining the Himalaya which have been built over this time (e.g., Raymo and Ruddiman, 1992). The details of how this links to silicate weathering on the continents remains unclear in part because of uncertainty in the partitioning of the Sr-flux from silicate and metacarbonate material (e.g., Edmond, 1992; Bickle et al., 2001, 2005).

Here we use the compositions of carbonate minerals from the upper oceanic crust to investigate the conditions within the crust during the time interval in which they were forming. We use their O-isotopic compositions to determine the temperature of the fluid they grew from and their Sr-isotopic composition to determine the amount of basalt dissolved into this fluid. We develop a simple model of fluid–rock reaction in the crust that allows us to invert these data to determine the temperature sensitivity of fluid–rock reaction. We find a strong temperature dependence of rock dissolution suggesting an important role for off-axis hydrothermal systems in controlling Earth's thermostat; i.e., when bottom water temperatures increase basalt dissolution rates increase and the drawdown of CO_2 into the upper oceanic crust increases. Modelling the decreased flux of unradiogenic Sr from off-axis hydrothermal systems into the ocean due to bottom water cooling over the last ~35 Myr shows that this is sufficient to explain most of the rise of seawater $^{87}Sr/^{86}Sr$ since this time.

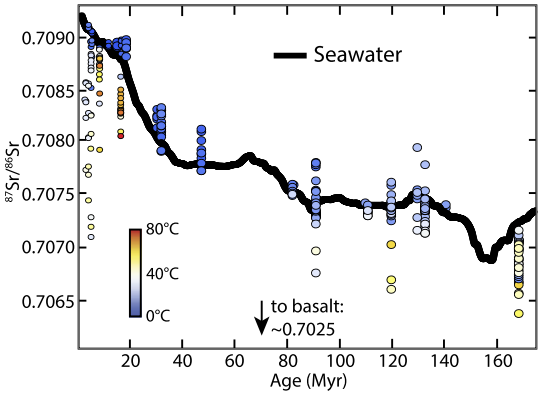

Fig. 1. Compilation of Sr-isotopic compositions of carbonates from the upper oceanic crust plotted as a function of the age of the crust they come from. Symbol colour reflects the temperature of carbonate precipitation using the carbonate O-isotope thermometer of Epstein et al. (1953) and the age dependence of the O-isotopic composition of seawater of Coggon et al. (2010). This is appropriate because the fluid $\delta^{18}O$ is little modified by fluid–rock reaction within the crust due to the high water-to-rock ratio (Anderson et al., 2013). The same fractionation factor was used for both aragonite and calcite because for many carbonate O- and Sr-isotope analyses the mineralogy is unknown, or mixed, and using the same fractionation factor only translates into a few degrees Celsius uncertainty. Note that higher carbonate precipitation temperatures are associated with lower $^{87}Sr/^{86}Sr$ due to larger amounts of basalt dissolution into the hydrothermal fluid. Larger symbols indicate those data used in the inversion while smaller symbols are data not used here due to coming from rapidly sedimented regions (see text for details). (For interpretation of the references to color in this figure legend, the reader is referred to the web version of this article.)

2. Determining the temperature dependence of rock dissolution

2.1. A carbonate Sr- and O-isotope compilation

In order to empirically determine the temperature dependence of fluid–rock reaction within off-axis hydrothermal systems we need tracers of both the fluid temperature and the amount of basalt that dissolved into the fluid. Carbonate O-isotope thermometry provides an estimate of the temperature of fluid–rock reaction and carbonate Sr isotope data provide information about the proportion of seawater and rock derived Sr in the fluid. We use a global compilation of the O- and Sr-isotopic compositions of carbonate minerals from the upper oceanic crust (Fig. 1) to quantify the temperature dependence of fluid–rock reaction. This is based on the compilation of Gillis and Coogan (2011) supplemented with data from Rausch et al. (2013) and new data, largely from the Troodos ophiolite ($n = 28$; 10 of which are unpublished data provided by K.M. Gillis), but also from drill cores in modern crust ($n = 5$; Supplementary Table 1). This global dataset was filtered to exclude locations were the sedimentation rate was >20 m Myr^{-1} (compared to a global average of 3.5 m Myr^{-1}; Anderson et al., 2012) because at such anomalously high sedimentation rates reactions within the sediment pile are likely to invalidate our assumption (see below) that the hydrothermal system is recharged by pristine seawater. Instead, a portion of the fluid recharging the hydrothermal system likely comes through the sediment and may be modified by reactions within the sedimentary pile. Samples from crustal sections that were sedimented rapidly mainly come from two distinct sedimentary environments.

The first group of rapidly sedimented sites are located under the equatorial sediment bulge where high productivity in the water column leads to rapid deposition of carbonate-rich sediments (mainly DSDP/ODP Holes 504B, 896A and 1256D; in the latter site the sedimentation rate was >30 m Myr^{-1} initially although

it has slowed as the crust drifted out of the equatorial bulge; Wilson et al., 2003). The pore fluids in these kinds of sediments can achieve very high Sr contents due to carbonate shell dissolution. For example, the pore fluids overlying Site 504 have up to seven times higher Sr contents than seawater (Mottl et al., 1983). At young crustal ages the carbonate sediments dissolving are also young, hence their Sr-isotopic composition is similar to that of contemporaneous seawater. Ingress of such Sr-rich pore fluid into the crust would mean that rock dissolution was far less effective in decreasing the Sr-isotopic composition of the hydrothermal fluid within the crust than if the fluid had the same Sr content as seawater. This suggestion is consistent with the observation that the rate of change of carbonate $^{87}Sr/^{86}Sr$ with increasing precipitation temperature is smaller at these sites than at normal sites (Fig. 2c).

The second group of rapidly sedimented sites involves locations that formed close to continental margins, dominantly from the Juan de Fuca plate. Here siliciclastic sediments derived from the largely juvenile continental crust of western N. America bury the oceanic crust soon after its formation. Because of the young, mantle derived, nature of most of the source rocks, these sediments have average Sr-isotopic compositions substantially lower than modern seawater (0.7071–0.7073; Carpentier et al., 2014). Reaction of pore fluid with these sediments will lower the fluid's $^{87}Sr/^{86}Sr$. Ingress of such pore fluid into the upper oceanic crust recharges the hydrothermal system with fluid with substantially lower $^{87}Sr/^{86}Sr$ than contemporaneous seawater meaning that less fluid–rock reaction within the lava pile is required to achieve a given hydrothermal fluid $^{87}Sr/^{86}Sr$. This is consistent with both: (i) the rapid but irregular decrease in pore fluid $^{87}Sr/^{86}Sr$ with depth in the sediment pile, alongside a small increase in pore fluid Sr content (Mottl et al., 2000), that suggests fluid-sediment reactions, and (ii) the very low $^{87}Sr/^{86}Sr$ values of some carbonates formed within the lavas in the Juan de Fuca plate that were precipitated at only moderate temperatures (Fig. 2d).

After filtering the data, 198 carbonates with both O- and Sr-isotopic composition measured remain; these come from crust ranging from 1.2 to 168 Myr old (Fig. 1; Table S1). The Sr-isotopic composition of these carbonates from "normal" altered upper oceanic crust depends mainly on: (i) the timing of carbonate mineral precipitation, through the secular variation in the Sr-isotopic composition of seawater; and (ii) the amount of basalt that had dissolved into the fluid that they precipitated from, because basalt dissolution adds unradiogenic Sr to the fluid. Carbonates that have $^{87}Sr/^{86}Sr$ higher than seawater of the age of the crust they form in (i.e. above the seawater curve in Fig. 1) must have formed at some point after the crust accreted, once the $^{87}Sr/^{86}Sr$ of seawater attained at least the measured carbonate $^{87}Sr/^{86}Sr$; this can be >15 Myrs in some cases. For a given crustal section, there is a trend of decreasing carbonate $^{87}Sr/^{86}Sr$ with increasing carbonate precipitation temperature (Figs. 1 and 2) indicating that increasing fluid temperature is a dominant control on the extent of rock dissolution (e.g., Staudigel et al., 1981; Butterfield et al., 2001; Coggon et al., 2004; Gillis and Coogan, 2011).

The minimum temperature of the fluid that the carbonate minerals grew from is similar to estimates of bottom water temperature, decreasing from $\sim 12 \pm 3\,^{\circ}C$ in the Mesozoic to $\sim 3 \pm 1\,^{\circ}C$ in the Cenozoic crustal sections (Fig. 3). The average temperature of carbonate precipitation varies in a given crustal section, and between locations, due to spatial and temporal variations in the thickness of overlying sediment, hydrology of the oceanic crust and timing of carbonate precipitation (e.g., Anderson et al., 2013). The difference between the minimum and average temperature of carbonate precipitation records the average amount that carbonate saturated fluid is heated in the crust and is $\sim 9\,^{\circ}C$ (Fig. 3). While there may be some difference between the average temperature of carbonate saturated fluids and the average temperature of hydrothermal fluid this difference is consistent with temperature changes estimated from hydrological models (e.g., Johnson and Pruis, 2003). This suggests that the average change in fluid temperature within the crust is similar in magnitude to the change in bottom water temperature over the last ~ 150 Myr; hence, changes in bottom water temperature are likely to be significant in controlling any temperature dependent processes within off-axis hydrothermal systems.

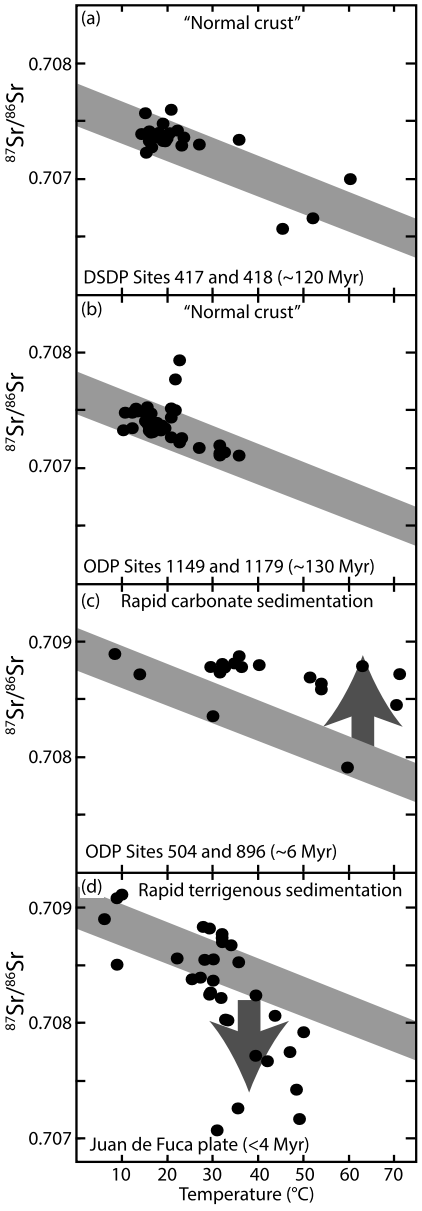

Fig. 2. Temperature dependence of carbonate Sr-isotopic composition from four regions; each region shows drill holes of a similar age (and hence seawater Sr-isotopic composition) and sedimentation history but these differ between regions. (a and b) Regions with typical abyssal sedimentation rates show similar decreases in $^{87}Sr/^{86}Sr$ with increasing fluid temperature due to dissolution of more rock Sr at higher temperatures. (c) Regions overlain by rapidly deposited carbonate sediments show less decrease in $^{87}Sr/^{86}Sr$ with increasing temperature than "normal" sites. This suggests either recharge of the system by Sr-rich pore fluids or diffusive Sr exchange between the pore fluids and crustal aquifer. (d) Regions overlain by rapidly deposited terrigenous sediments show more decrease in $^{87}Sr/^{86}Sr$ with increasing temperature than "normal" sites, consistent with recharge of the system by pore fluids with $^{87}Sr/^{86}Sr$ lower than seawater. See text for discussion. The gray band has the same slope in all panels and is drawn based on the data in (a) and (b) simply to emphasize the difference between these data and that shown in (c) and (d).

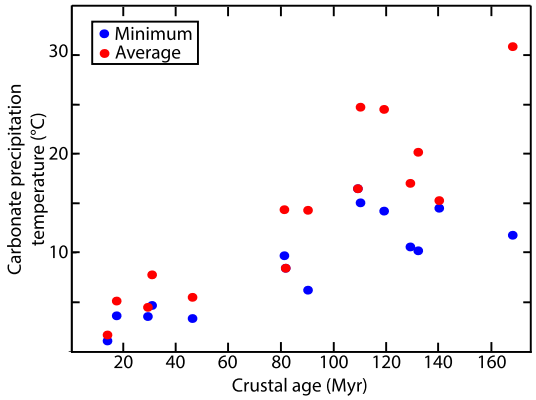

Fig. 3. Variation of the minimum and average temperature of carbonate precipitation in the upper oceanic crust with crustal age. On average, carbonates from the upper oceanic crust are precipitated at temperatures ~9 °C warmer than contemporaneous bottom water, approximated by the minimum precipitation temperature.

2.2. A box model for an off-axis hydrothermal system

With the aim of determining the temperature dependence of fluid–rock reaction in off-axis hydrothermal systems we developed a model to predict carbonate Sr-isotopic composition as a function of fluid temperature and then inverted this to determine the probability density for the controlling parameters. We developed the simplest possible realistic model of the evolution of the hydrothermal fluid $^{87}Sr/^{86}Sr$ during fluid–rock reaction in an off-axis hydrothermal system. We assume a single box model in which bottom water enters the crust through an outcrop, flows through the crust reacting at some average temperature and precipitates secondary minerals, and discharges back into the ocean (Fisher and Becker, 2000; Anderson et al., 2012). Isotope exchange within the off-axis hydrothermal system is assumed to follow first-order kinetics (Lasaga, 1998) such that, under the assumption of fixed concentrations of Sr in the rock and fluid, we can write:

$$\frac{d(^{87}Sr/^{86}Sr_{hydro})}{dt} = k\left(^{87}Sr/^{86}Sr_{basalt} - {}^{87}Sr/^{86}Sr_{hydro}\right) \quad (1)$$

leading to:

$$^{87}Sr/^{86}Sr_{hydro} = \exp[-kt]\left(^{87}Sr/^{86}Sr_{SW} - {}^{87}Sr/^{86}Sr_{basalt}\right) + {}^{87}Sr/^{86}Sr_{basalt} \quad (2)$$

where t = time; subscript SW = seawater; subscript $hydro$ = the composition of the hydrothermal fluid and hence the carbonate minerals precipitated from it; and subscript $basalt$ = fresh rock Sr-isotopic ratio, assumed to be 0.7025 for all modern oceanic sites and 0.7035 for the Troodos ophiolite. Eq. (1) is equivalent to assuming the rate of fresh basalt dissolution, and hence release of unradiogenic Sr into the hydrothermal fluid, is constant. Variation in the Sr content of seawater in the past can be accounted for by mass balance given that the fraction of basaltic Sr leached into the fluid is defined by Eq. (1) and under the assumption that the Sr content of the fluid stays constant during fluid–rock reaction (Supplementary material). Higher paleo-seawater Sr contents simply act to dilute the unradiogenic Sr leached from the rock; e.g., doubling the seawater Sr content leads to a doubling of the amount of basaltic Sr that must be leached to achieve a given hydrothermal fluid $^{87}Sr/^{86}Sr$. The reaction rate constant (k) for isotopic exchange is assumed to follow a simple Arrhenius relationship and can be written as:

$$k = B\exp\left[\frac{-C}{RT}\right] \quad (3)$$

where B and C are unknown constants, T is absolute temperature (Kelvin) and R is the gas constant. The constant C can be thought of as an apparent activation energy for rock dissolution and Sr release. However, the value extracted from modelling natural data may depend on numerous processes and will not necessarily match experimental measurements of the activation energy for mineral dissolution. We assume that the average duration of fluid–rock reactions (t) is the same in different settings and use a normalized average value of 1 for t. Hence the constant B is also dimensionless (as is k) and would need to be divided by the average duration of fluid–rock reactions to convert it into units of reciprocal time. It is possible that reaction rates may vary along the flow path due to changes in fluid composition modifying the saturation state of the relevant phases. Both because we aim to use the simplest possible model, and because the (very limited) existing data do not suggest large changes in fluid composition within normal crust (Wheat and Fisher, 2008), we do not consider this in the modelling presented here.

Because the Sr-isotopic composition of seawater has changed over time, and we do not know how long after crustal accretion a given carbonate mineral formed, we do not know the Sr-isotopic composition of seawater at the time of carbonate formation; thus we cannot directly solve Eq. (2). To overcome this we use a model to describe the rate of carbonate precipitation as a function of time after crustal accretion and hence the probability of seawater having any given $^{87}Sr/^{86}Sr$ at the time of carbonate formation. We assume an exponential decrease in the rate of carbonate precipitation after crustal accretion for the following reasons. Firstly, the difference between measured conductive heat flow at the seafloor and predicted heat flow from lithospheric cooling models show that the amount of heat carried by hydrothermal circulation, and the calculated volume flux of fluid carrying this heat, decrease near-exponentially with increasing crustal age (Stein and Stein, 1994). Secondly, radiometric dating of secondary minerals formed in off-axis hydrothermal systems suggest that their formation rate decreases near exponentially with time (Staudigel, 2014). The fraction of the total amount of carbonate that would form that has been precipitated at any given time after crustal formation (f_{carb}) is given:

$$f_{carb} = 1 - \exp(-\tau A) \quad (4)$$

where τ = time constant for carbonate precipitation (Myr^{-1}) and A = time after crustal accretion (Myr). Thus, when solving Eq. (2) for the probability density of hydrothermal fluid $^{87}Sr/^{86}Sr$, a distribution of $^{87}Sr/^{86}Sr_{SW}$ is used determined from the value of τ and the variation in $^{87}Sr/^{86}Sr_{SW}$ following the time of crustal accretion. If τ is very large all carbonate forms almost synchronously with crustal accretion and $^{87}Sr/^{86}Sr_{SW}$ in Eq. (2) would be that of seawater at the time of crust formation. In contrast, if τ is very small carbonate forms at an almost constant rate after crust accretion and all observed values of $^{87}Sr/^{86}Sr_{SW}$ following crustal accretion would be similarly probable (see below and Fig. 4).

2.3. Model carbonate $^{87}Sr/^{86}Sr$ probability density

Eq. (2) can be solved to produce a probability density of hydrothermal fluid (and hence carbonate) Sr-isotopic compositions given values for the three unknown parameters (τ, B, C), the temperature of fluid–rock reaction (T in Eq. (3)) and a record of seawater Sr-content and Sr-isotopic composition following crustal formation. In computing the hydrothermal fluid $^{87}Sr/^{86}Sr$ probability density the temperature of fluid–rock reaction was assumed to match the temperature determined by carbonate O-isotope thermometry ($T_{measured}$) but a 1σ uncertainty of 3 °C was assigned to this (with a minimum temperature cut-off at 0 °C). This uncertainty reflects the possibility that fluid–rock reaction and carbonate

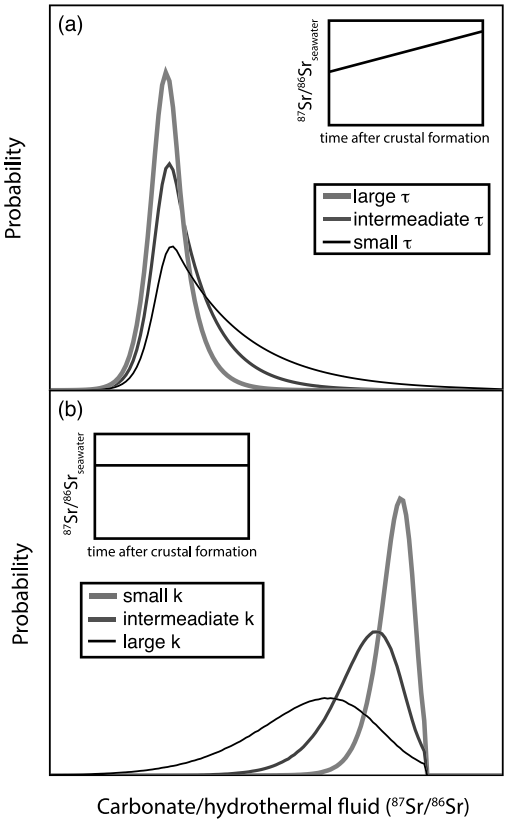

Fig. 4. Cartoon examples of how the unknown model parameters control the probability density of a carbonate having a given $^{87}Sr/^{86}Sr$. (a) Assuming the $^{87}Sr/^{86}Sr$ of seawater increases monotonically with time after crustal formation, larger values of the time constant for carbonate precipitation (τ) lead to tighter $^{87}Sr/^{86}Sr$ probability densities. (b) Assuming the $^{87}Sr/^{86}Sr$ of seawater remains constant, a larger reaction rate constant (k) leads to a broader $^{87}Sr/^{86}Sr$ probability density extending to lower $^{87}Sr/^{86}Sr$ values.

precipitation may not have occurred at exactly the same temperature, as well as the uncertainty in the thermometer. Additionally, we assigned a 1σ uncertainty of 0.5 to the normalized time that the fluid was in the crust (t); this is based on models of the variation of flow path lengths in off-axis hydrothermal systems (Anderson et al., 2012). The seawater Sr-isotope curve was taken from a fit through the data of Veizer et al. (1999). The time evolution of the Sr-content of seawater was taken from a fit through the compilation in Fig. 3 of Coogan (2009) as follows: 0–55 Ma: $Sr = 0.11age + 7.8$; 56–100 Ma: $Sr = 0.29age - 1.9$; and >100 Ma: $Sr = 27$, where age is in Myr and Sr contents are in ppm.

Examples of how the unknown model parameters (τ, B, C) affect the probability density of carbonate Sr-isotopic compositions are shown in Fig. 4. Small values of the time constant for carbonate deposition (τ) lead to slow carbonate precipitation rates and the Sr-isotopic composition of seawater recharging the crustal aquifer can have a large range of compositions (assuming seawater $^{87}Sr/^{86}Sr$ changes in the time following crustal accretion). Large values of τ, in contrast, lead to rapid carbonate precipitation and the fluid recharging the crust has an isotopic composition similar to that of seawater at the age of the crust (Fig. 4a). The parameters B and C combined with the fluid temperature define the reaction rate constant (k; Eq. (3)). Increasing k leads to an increase in the maximum amount of basaltic Sr that can be dissolved into the fluid. This means that large values of k lead to broader fluid $^{87}Sr/^{86}Sr$ probability density that reach lower absolute $^{87}Sr/^{86}Sr$ values (Fig. 4b).

To produce model distributions of the Sr-isotopic composition of the hydrothermal fluid for any given values of the three unknown parameters, to compare to the data, 1000 Monte Carlo simulations were run. These used random draws from the Gaussian probability density of the temperature of carbonate precipitation ($T_{measured} \pm 3\,°C$; see above) and duration of fluid–rock reaction ($t = 1 \pm 0.5$; see above). Because 1000 draws is insufficient to precisely define the probability density at low probabilities, we extrapolate the high-temperature (low $^{87}Sr/^{86}Sr$) side of the distribution assuming a Gaussian tail to the distribution. This is computed using the lowest Sr-isotopic composition of seawater after the time of crustal formation as this provides the lowest possible value of $^{87}Sr/^{86}Sr_{hydro}$ for any given temperature. The resulting probability densities resemble those in Fig. 4 but are not as smooth due to the complex temporal variation of $^{87}Sr/^{86}Sr$ in seawater. These probability densities are then compared to the data point to define the model's probability for that data point. The probability of the model (i.e. any given set of values of τ, B and C) is calculated from the product of the probabilities for each data point, across all 198 data, which defines the joint probability density given independent samples.

2.4. Inversion procedure

A given set of values of τ, B and C constitutes a given model which has a given probability calculated as just described. To invert the data to determine the best estimates of the values of τ, B and C, and their uncertainties, we require an efficient sampling method to search parameter space. To achieve this a numerical Bayesian inference procedure was used. In this the unknown model parameters (τ, B, C) were treated as random variables constrained by the data and by prior bounds on their possible values (i.e., physically-reasonable limits on the parameter space), and the inversion estimates the posterior probability density (PPD). The PPD was estimated by searching the parameter space using the Markov-chain Monte Carlo method of Metropolis–Hastings sampling (Gilks et al., 1996), in which random parameter perturbations are proposed and then accepted or rejected according to a probabilistic condition (Metropolis–Hastings criterion). For efficiency, parameter perturbations were applied in a principal-component parameter space drawn from a linearized approximation to the PPD (Dosso and Wilmut, 2008). To ensure a sufficiently wide search of parameter space, multiple interacting Markov chains were run within a parallel-tempering formulation (Earl and Deem, 2005; Dosso et al., 2012). This provides both broad searching of the entire parameter space and efficient concentrated searching of the high probability regions. The end result is a close approximation to the result of determining the probability of models with every possible combination of these three parameters.

2.5. Results of the inversion

The numerical inversion defines the probability density of the three unknown model parameters (Fig. 5). The best estimate of τ is 0.107 ± 0.012 Myr^{-1} indicating that 80% of carbonates are precipitated within 15 Myr (Fig. 5a) of crustal accretion, consistent with radiometric ages of secondary minerals in altered oceanic crust (Staudigel, 2014). The best estimate of the apparent activation energy for rock dissolution (C) is 92 ± 7 kJ mol^{-1} (Fig. 5b). The apparent activation energy extracted from the modelling reflects the integrated temperature dependence of numerous processes. However, it is noteworthy that the value is within the range of experimentally determined activation energies for dissolution of the dominant minerals in the oceanic crust (plagioclase: 42–81 kJ mol^{-1} and pyroxene: 41–95 kJ mol^{-1}; Brantley and Olsen, 2014).

These results demonstrate that, during the time of CO_2 consumption by the oceanic crust, there is a strong temperature de-

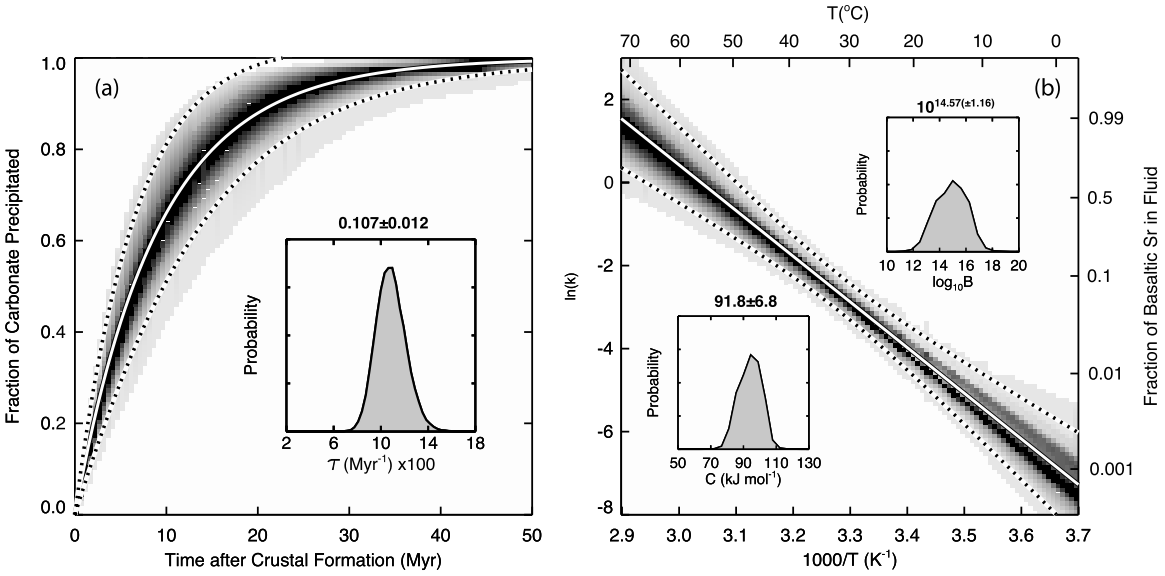

Fig. 5. Results of the inversion. (a) Cumulative fraction of carbon uptake by the oceanic crust as a function of time after crustal formation. (b) Arrhenius plot showing the temperature dependence of the reaction rate constant (k) for Sr release from the crust and the fraction of basaltic Sr in the fluid at any given temperature (assuming modern seawater Sr concentration). The gray-scale shading represents the probability density (uncertainty distribution) normalized independently at each age (in a) and temperature (in b), with the white line representing the mean estimate and the dashed lines 2σ uncertainty bounds around this estimate. Insets show marginal probability density functions for the three model parameters discussed in the text. Marginal probability densities are relatively simple and symmetric, and, hence, are well represented by their means and standard deviations, which are the values used here. As expected, the values of B and C correlate almost perfectly in high probability models as these play off each other in determining k for a given temperature (Eq. (3)).

pendence of the rate of rock dissolution. For example, an increase in bottom water temperature from 2 to 12 °C would lead to a factor of four increase in the rate of Sr release due to basalt dissolution. This strong temperature sensitivity of the rate of rock dissolution is consistent with the large difference between the mass of carbonate minerals found in late Mesozoic ocean crust (altered under warm bottom water conditions of ~10–15 °C) and late Cenozoic oceanic crust (altered under cool bottom water conditions of ~2–5 °C). Gillis and Coogan (2011) show that the C-content of the former is roughly five times higher than that of the latter, requiring fluid–rock reactions generated roughly five times more alkalinity under the warmer conditions (Coogan and Gillis, 2013). Note that the precipitation of the vast majority of the carbonates within ~ 20 Myr of crustal accretion (Fig. 5a) indicates that this difference does not reflect a longer lifetime of alteration for the Mesozoic sites. Thus, both the Sr-isotopic composition of the carbonate minerals, and their abundance in altered upper oceanic crust, are consistent with a 10–15 °C change in bottom water temperature leading to a 4 to 5 fold increase in the extent of rock dissolution in off-axis hydrothermal systems.

Because the Sr content of paleoseawater is uncertain, we also evaluated a model in which the Sr concentration of seawater was held constant at the modern value. This constant-Sr model produced a significantly worse fit to the data, with the difference between the minimum misfit (negative log-likelihood) for the two models being 11.7; i.e. in terms of the likelihood ratio, the best fitting model with variable seawater Sr content is ~120,000 times more likely than that with fixed seawater Sr content. The best estimates of the parameters are similar for this model with no change in Sr content ($\tau = 0.091 \pm 0.011$ Myr^{-1}; $C = 74 \pm 5$ kJ mol^{-1}; Log(B) $= 11.3 \pm 0.8$) to those extracted from the model with changing seawater Sr content although with a somewhat smaller apparent activation energy for rock dissolution (74 ± 5 kJ mol^{-1} versus 92 ± 7 kJ mol^{-1}). Additional sensitivity tests, performed as grid searches, showed that changing the standard deviation on the normalized duration of fluid–rock reaction within the crust (0.3 and 0.5) and the standard deviation of the temperature of fluid–rock reaction around the temperature of carbonate precipitation calculated from the carbonate Sr-isotopic composition (1.5 and 3 °C) made little difference to the parameter estimates; hence, the results appear to be robust.

3. Implications of a strong temperature-dependence of ocean crust alteration

The O- and Sr-isotopic compositions of carbonates precipitated in seafloor off-axis hydrothermal systems demonstrate that they formed early in the lifetime of the crust (Fig. 5a) and that there is a strong temperature-dependence of the rate of rock dissolution (Fig. 5b). These results have important implications for both the long-term C-cycle and for interpreting the secular variation in the Sr-isotopic composition of seawater.

3.1. Modelling the Sr-isotopic evolution of seawater

The temperature dependence of the Sr-isotopic composition of the hydrothermal fluid determined above (Fig. 5b) allows us to calculate the change in the flux of unradiogenic Sr into the ocean due to a change in ocean bottom water temperature. In turn this allows the impact of changing bottom water temperature on secular variations in the Sr-isotopic composition of seawater to be calculated. We take the evolution of bottom water temperature from Lear et al. (2000) and model the evolution of the Sr-isotopic composition of seawater using the standard approach except that we include a temperature dependence of the Sr-isotopic composition of the off-axis hydrothermal flux. The Sr content of the off-axis hydrothermal fluid is assumed to match that of seawater. The change in the Sr content of seawater is determined from:

$$\frac{dN}{dt} = F_{riv} + F_{hThy} + F_{lThy} + F_{dia} + F_{carb} \quad (5)$$

where N = number of moles of Sr in the ocean; t = time (yr); F = flux (mol yr^{-1}); riv = river; $hThy$ = high temperature, ridge axis, hydrothermal systems; $lThy$ = low temperature, off-axis, hydrothermal systems; dia = diagenetic fluids; $carb$ = sedimentary Sr sink largely into carbonates. F_{carb} is adjusted to make dN/dt fit

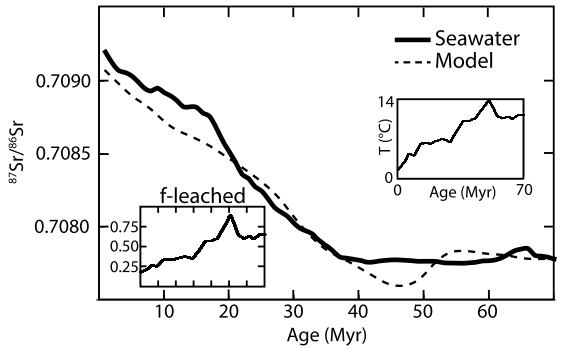

Fig. 6. Model of the effect of cooling bottom water on the evolution of seawater $^{87}Sr/^{86}Sr$. Fluxes into and out of the ocean, and their isotopic compositions, were held constant except the isotopic composition of the low-temperature hydrothermal flux. This was varied with bottom water temperature (see text for details). Bottom water temperature (Lear et al., 2000) shows a progressive, but uneven, cooling over the Cenozoic (inset) leading to a decreased hydrothermal flux of unradiogenic Sr and hence an increase in seawater $^{87}Sr/^{86}Sr$. The fraction of the basaltic Sr leached from the upper oceanic crust (formed with 1×10^{10} mol of Sr yr^{-1}) as function of time is shown in the lower left inset (f-leached). In reality less Sr is likely leached from the upper oceanic crust as some will be supplied from deeper crustal levels.

the change in Sr concentration in seawater described above (although using a constant seawater Sr content has negligible effect on the result). The change in the Sr-isotopic composition of seawater is calculated from:

$$N\frac{dR}{dt} = F_{riv}(R_{riv} - R_{SW}) + F_{hThy}(R_{hThy} - R_{SW}) + F_{lThy}(R_{lThy} - R_{SW}) + F_{dia}(R_{dia} - R_{SW}) \quad (6)$$

where R = Sr-isotopic ratio. The sedimentary carbonate sink is ignored in Eq. (6) because this has the same Sr-isotopic composition as the ocean. We solve Eqs. (5) and (6) at 10,000 yr time steps in the models shown in Fig. 6 but shorter time steps make no difference to the results.

We are interested in what proportion of the change in seawater Sr-isotopic composition over the last 70 Myrs comes from changes in the extent of low-temperature alteration of the oceanic crust due to changes in bottom water temperature. Thus, we ran a model forced only by the effect of changes in bottom water temperature on the Sr-isotopic composition of the flux from the low-temperature, off-axis, hydrothermal systems (Eq. (2)). To achieve this we held the Sr fluxes from, and average Sr-isotopic ratio of, the river input constant. We also set the Sr fluxes from diagenetic pore fluids, and both low and high temperature hydrothermal systems, to be constant. The Sr-isotopic compositions of high-temperature hydrothermal fluids and diagenetic fluids were fixed relative to contemporaneous (model) seawater Sr-isotopic composition. The Sr-isotopic composition of high-temperature hydrothermal fluid was a mix of 80% basalt (0.7025) and 20% of the model seawater Sr-isotopic composition at that model time (Coogan and Dosso, 2012). A similar approach was taken for the Sr-isotopic composition of diagenetic fluids except that, due to contributions of Sr to these from both the underlying oceanic crust and the sediments, a constant offset of their Sr-isotopic ratio was assumed (0.00075 lower than the model seawater Sr-isotopic composition; Elderfield and Gieskes, 1982). The exact value used makes little difference due to the small diagentic Sr flux. The Sr-isotopic composition of low-temperature hydrothermal fluids was then calculated from Eq. (2) using the estimates of B and C from the inversion of the carbonate O- and Sr-isotopic compositions (Fig. 5b) and a hydrothermal fluid temperature equal to the measured value (~9 °C; Fig. 3) higher than that of the bottom seawater. The same change in temperature of the fluid within the crust was used to determine the hydrothermal fluid flux based on the requirement that it carries the 5 TW of heat transported by hydrothermal fluids in crust between 2 and 20 Myr in age (Stein and Stein, 1994). The use of this average temperature increase provides a first approximation to the 'chemically significant' off-axis hydrothermal flux; more sophisticated models will have to consider the (poorly constrained) temperature distribution of hydrothermal fluid rather than simply the average. All input values and sources are listed in Supplementary Table S2.

A problem for all models of the Sr-isotopic composition of seawater comes from uncertainty in the steady-state river Sr flux. The modern river Sr flux is generally thought to be far higher than any plausible steady-state flux (Davis et al., 2003; Vance et al., 2009) possibly due to glacial–interglacial (Vance et al., 2009) or anthropogenic (e.g., Sen and Peucker-Ehrenbrink, 2012) perturbations. Alternatively, it has been suggested that the modern river flux has been over-estimated and is only ~55% of that reported in earlier studies (Allegre et al., 2010). Additionally, recent increases in the Sr-isotopic composition of rivers draining the Himalaya may lead to the measured flux of radiogenic Sr being higher than at steady state (Rahaman et al., 2011). To work around this uncertainty we set the river Sr flux to that required to balance the oceanic Sr-isotopic budget at the start of the model (70 Ma) holding the river Sr-isotopic ratio at the modern value (0.7114; Vance et al., 2009). The resulting river Sr flux is 1.2×10^{10} mol yr^{-1} compared to other recent estimates of $\sim 1.6 \times 10^{10}$ (Allegre et al., 2010) and $\sim 1.7 \times 10^{10}$ (Vance et al., 2009) mol yr^{-1}.

The modelled time-evolution of the Sr-isotopic composition of seawater over the last 70 Myr, due to changes in the flux of unradiogenic Sr into the ocean from off-axis hydrothermal circulation driven by changing bottom water temperature, is shown in Fig. 6. This model seawater $^{87}Sr/^{86}Sr$ curve is remarkably close to fitting the observed variation despite the model clearly being overly simplistic. In particular the model reproduces the rapid increase in seawater $^{87}Sr/^{86}Sr$ starting in the Late Eocene that coincides with Antarctic cooling (Zachos et al., 1999). Even if the temperature dependence of Sr-leaching from the oceanic crust determined here is over-estimated, it is clear that a decreased hydrothermal flux must have played a significant role in the increase in seawater $^{87}Sr/^{86}Sr$ as bottom water cooled since the Late Eocene. This model contrasts with the standard explanation that invokes an increased input of radiogenic Sr from rivers, largely draining the Himalaya, during this time (e.g., Raymo and Ruddiman, 1992; Richter et al., 1992; Bickle et al., 2001, 2005). It seems likely that changes in bottom water temperature also impact the off-axis hydrothermal flux, and its isotopic composition, for many other species of interest in studies of the Earth system (e.g., Li, B, O, Mg, K, Ca). The common approach of assigning secular variation in seawater composition largely, or solely, to environmentally driven changes in subaerial processes needs reconsidering.

3.2. Implications for the long-term C-cycle

Average ocean bottom water temperature is sensitive to changes in global climate (e.g., Lear et al., 2000; Zachos et al., 2001) due to changes in surface temperature in regions of deep water formation (e.g., Pagani et al., 2014). Warming of Earth's climate leads to higher temperature seawater entering off-axis hydrothermal systems and hence more rapid rock dissolution and greater CO_2 consumption by these systems (Fig. 7). In turn this provides a negative feedback on CO_2-induced greenhouse warming and acts to stabilize global climate. Changes in bottom water temperature of $\geq$10 °C between the late Mesozoic and late Cenozoic are similar to the average increase in fluid temperature within the crust (~9 °C; Fig. 3); i.e. changes in bottom water temperature play a major role in controlling fluid temperature and hence fluid–rock reaction rates in off-axis hydrothermal systems. As noted above, the observed factor of five higher C-content of late Mesozoic upper oceanic

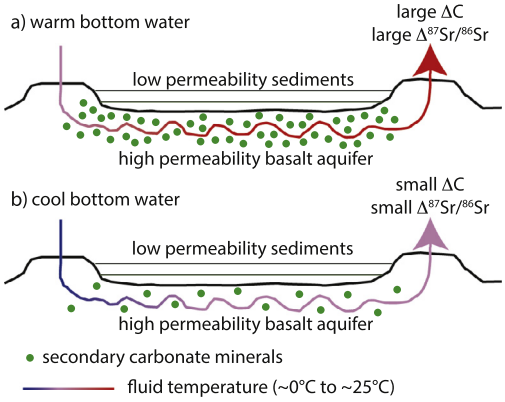

Fig. 7. Cartoon illustrating the proposed model. (a) When bottom water is warm (e.g., late Mesozoic) the water within off-axis hydrothermal systems is relatively warm, and reacts extensively with the crust. In turn this drives precipitation of significant amounts of carbonate minerals and decreases the $^{87}Sr/^{86}Sr$ of the fluid. Discharge of this modified fluid back into the ocean acts as a sink for seawater CO_2 (at near constant alkalinity) and to lower seawater's $^{87}Sr/^{86}Sr$. (b) During cooler periods (e.g., late Cenozoic) the crustal aquifer is recharged by cooler water leading to less extensive fluid–rock reaction and less modification of seawater composition. The hydrological regime shown is illustrative of flow between outcrops but this is not meant to imply this is the only hydrological regime relevant to the processes discussed here.

crust, relative to late Cenozoic aged crust (Alt and Teagle, 1999; Gillis and Coogan, 2011), is consistent with CO_2 consumption in off-axis hydrothermal systems providing a strong temperature-dependent feedback on the long-term C-cycle.

In the standard view of the long-term carbon cycle, cooling over the last 50 Myr would be expected to lead to decreased chemical weathering of the continents. However, there is little evidence for decreased continental chemical weathering during this time. Instead, the Sr- and Li-isotopic ratios of seawater both increase (Veizer et al., 1999; Misra and Froelich, 2012) which could be interpreted as indicating increased continental chemical weathering perhaps due to tectonic uplift (e.g., Raymo and Ruddiman, 1992). Numerous models have been put forward to explain this "Cenozoic isotope-weathering paradox". These include changing continental weatherability (e.g., Raymo and Ruddiman, 1992), increased metamorphic CO_2 degassing (Bickle, 1998), changing the partitioning of weathering between old continents and ocean islands (Li and Elderfield, 2013) and sulphide oxidation induced CO_2 release (Torres et al., 2014). While all of these processes, and others, may play important roles in the long-term C-cycle, a strong temperature-dependent feedback on seafloor CO_2 consumption would resolve this paradox (of course, as discussed in Section 3.1, the interpretation of the isotope records could change too). In this model, decreasing bottom water temperature would decrease CO_2 consumption by the oceanic crust irrespective of how other factors affected rates of continental chemical weathering (Fig. 7). For example, an uplift-induced increase in physical weathering of the continents could lead to increased continental chemical weathering and hence increased CO_2 drawdown, with the CO_2 cycle balanced by decreased carbonate mineral formation in the oceanic crust.

4. Summary and conclusions

We used the Sr- and O-isotopic compositions of carbonates precipitated at low temperature in off-axis hydrothermal systems to rigorously quantify the temperature-dependence of rock dissolution in these systems. The strong temperature dependence we find is consistent with the observed higher abundance of carbonate minerals in upper oceanic crust altered under the warmer bottom water condition of the late Mesozoic than under the cooler bottom water conditions of the late Cenozoic (Gillis and Coogan, 2011). Fig. 7 summarizes the effect of changing bottom water temperature on the chemical fluxes associated with off-axis hydrothermal systems discussed here. As bottom water temperature increases so does the temperature in the upper oceanic crust in the off-axis. This higher temperature leads to increased rates of rock dissolution, greater alkalinity generation, and the leaching of substantially more unradiogenic Sr from the rock than under cooler conditions. In turn, larger masses of carbonate minerals are precipitated in the crust, and the fluid vented back into the ocean is more C-depleted, and has a lower $^{87}Sr/^{86}Sr$ relative to contemporaneous seawater. This dependence of the chemical fluxes from seafloor hydrothermal systems on bottom water temperature must be important for other species as well as C and Sr and needs considering in Earth system models.

Perhaps it should be no surprise that seafloor hydrothermal systems appear to play an important role in the long-term carbon cycle (Francois and Walker, 1992; Brady and Gislason, 1997; Gillis and Coogan, 2011; Coogan and Gillis, 2013). The oceanic crust is made of more reactive rock (basaltic) than average upper continental crust (granitic), is constantly being regenerated, and is always immersed in water unlike continental crust. The sensitivity of bottom water temperature to global climate provides a simple feedback mechanism for off-axis hydrothermal systems to respond to changes in environmental conditions. We do not mean to suggest that other processes, such as continental chemical weathering, play no role in the long-term carbon cycle, but it seems clear that off-axis hydrothermal systems play an important, and generally overlooked, role.

Acknowledgements

Mike Bickle and an anonymous reviewer are thanked for journal reviews that improved the manuscript and Kathy Gillis and Jay Cullen are thanked for comments on an early version of the text. LAC and SED acknowledge support from NSERC Discovery grants. Analytical work was supported by NSERC Discovery grant 283238.

Appendix A. Supplementary material

Supplementary material related to this article can be found online at http://dx.doi.org/10.1016/j.epsl.2015.01.027.

References

Allegre, C.J., Louvat, P., Gaillardet, J., Meynadier, L., Rad, S., Capmas, F., 2010. The fundamental role of island arc weathering in the oceanic Sr isotope budget. Earth Planet. Sci. Lett. 292, 51–56.

Alt, J.C., Teagle, D.A.H., 1999. The uptake of carbon during alteration of ocean crust. Geochim. Cosmochim. Acta 63, 1527–1535.

Anderson, B.W., Coogan, L.A., Gillis, K.M., 2012. The role of outcrop-to-outcrop fluid flow in off-axis oceanic hydrothermal systems under abyssal sedimentation conditions. J. Geophys. Res. 117. http://dx.doi.org/10.1029/2011JB009052.

Anderson, B.W., Gillis, K.M., Coogan, L.A., 2013. A hydrologic model for the uppermost oceanic crust constrained by temperature estimates from carbonate minerals. J. Geophys. Res. 118, 3917–3930.

Berner, R.A., 2004. The Phanerozoic Carbon Cycle. Oxford University Press, New York.

Berner, R.A., Caldeira, K., 1997. The need for mass balance and feedback in the geochemical carbon cycle. Geology 25, 955–956.

Berner, R.A., Lasaga, A.C., Garrels, R.M., 1983. The carbonate–silicate geochemical cycle and its effect on atmospheric carbon dioxide over the past 100 million years. Am. J. Sci. 283, 641–683.

Bickle, M.J., 1998. The need for mass balance and feedback in the geochemical carbon cycle: comment. Geology 26, 477–478.

Bickle, M.J., Chapman, H.J., Bunbury, J., Harris, N.B.W., Fairchild, I.J., Ahmad, T., Pomies, C., 2005. Relative contributions of silicate and carbonate rocks to riverine Sr fluxes in the headwaters of the Ganges. Geochim. Cosmochim. Acta 69, 2221–2240.

Bickle, M.J., Harris, N.B.W., Bunbury, J.M., Chapman, H.J., Fairchild, I.J., Ahmad, T., 2001. Controls on the $^{87}Sr/^{86}Sr$ ratio of carbonates in the Garhwal Himalaya, headwaters of the Ganges. J. Geol. 109, 737–753.

Brady, P.V., Gislason, S.R., 1997. Seafloor weathering controls on atmospheric CO_2 and global climate. Geochim. Cosmochim. Acta 61, 965–973.
Brantley, S.L., Olsen, A.A., 2014. Reaction kinetics of primary rock-forming minerals under ambient conditions. In: Treatise on Geochemistry. 2nd edition, pp. 69–113.
Butterfield, D.A., Nelson, B.K., Wheat, C.G., Mottl, M.J., Roe, K.K., 2001. Evidence for basaltic Sr in mid-ocean ridge-flank hydrothermal systems and implications for the global Sr-isotope balance. Geochim. Cosmochim. Acta 65, 4141–4153.
Caldeira, K., 1995. Long-term control of atmospheric carbon-dioxide – low-temperature sea-floor alteration or terrestrial silicate–rock weathering. Am. J. Sci. 295, 1077–1114.
Carpentier, M., Weis, D., Chauvel, C., 2014. Fractionation of Sr and Hf isotopes by mineral sorting in Cascadia Basin terrigenous sediments. Chem. Geol. 380, 67–82.
Coggon, R.M., Teagle, D.A.H., Cooper, M.J., Vanko, D.A., 2004. Linking basement carbonate vein compositions to porewater geochemistry across the eastern flank of the Juan de Fuca Ridge, ODP Leg 168. Earth Planet. Sci. Lett. 219, 111–128.
Coggon, R.M., Teagle, D.A.H., Smith-Duque, C.E., Alt, J.C., Cooper, M.J., 2010. Reconstructing past seawater Mg/Ca and Sr/Ca from mid-ocean ridge flank calcium carbonate veins. Science 327, 1114–1117.
Coogan, L.A., 2009. Altered oceanic crust as an inorganic record of paleoseawater Sr concentration. Geochem. Geophys. Geosyst. 10. http://dx.doi.org/10.1029/2008GC002341.
Coogan, L.A., Dosso, S., 2012. An internally consistent, probabilistic, determination of ridge-axis hydrothermal fluxes from basalt-hosted systems. Earth Planet. Sci. Lett. 323, 92–101.
Coogan, L.A., Gillis, K.M., 2013. Evidence that low-temperature oceanic hydrothermal systems play an important role in the silicate–carbonate weathering cycle and long-term climate regulation. Geochem. Geophys. Geosyst. 14, 1771–1786.
Davis, A.C., Bickle, M.J., Teagle, D.A.H., 2003. Imbalance in the oceanic strontium budget. Earth Planet. Sci. Lett. 211, 173–187.
Dosso, S.E., Holland, C.W., Sambridge, M., 2012. Parallel tempering for strongly nonlinear geoacoustic inversion. J. Acoust. Soc. Am. 132, 3030–3040.
Dosso, S.E., Wilmut, M.J., 2008. Uncertainty estimation in simultaneous Bayesian tracking and environmental inversion. J. Acoust. Soc. Am. 124, 82–97.
Earl, D.J., Deem, M.W., 2005. Parallel tempering: theory, applications, and new perspectives. Phys. Chem. Chem. Phys. 7, 3910–3916.
Edmond, J.M., 1992. Himalayan tectonics, weathering processes, and the strontium isotope record in marine limestones. Science 258, 1594–1597.
Elderfield, H., Gieskes, J.M., 1982. Sr-isotopes in interstitial waters of marine-sediments from Deep-Sea Drilling Project cores. Nature 300, 493–497.
Epstein, S., Buchsbaum, R., Lowenstam, H.A., Urey, H.C., 1953. Revised carbonate-water isotopic temperature scale. Geol. Soc. Am. Bull. 64, 1315–1325.
Fisher, A.T., Becker, K., 2000. Channelized fluid flow in oceanic crust reconciles heat-flow and permeability data. Nature 403, 71–74.
France-Lanord, C., Derry, L.A., 1997. Organic carbon burial forcing of the carbon cycle from Himalayan erosion. Nature 390, 65–67.
Francois, L.M., Walker, J.C.G., 1992. Modelling the Phanerozoic carbon cycle and climate: constraints from the $^{87}Sr/^{86}Sr$ isotopic ratio of seawater. Am. J. Sci. 292, 81–135.
Gilks, W.R., Richardson, S., Spiegelhalter, G.J., 1996. Markov Chain Monte Carlo in Practice. Chapman and Hall.
Gillis, K.M., Coogan, L.A., 2011. Secular variation in carbon uptake into the ocean crust. Earth Planet. Sci. Lett. 302, 385–392.
Johnson, H.P., Pruis, M.J., 2003. Fluxes of fluid and heat from the oceanic crustal reservoir. Earth Planet. Sci. Lett. 216, 565–574.
Lasaga, A.C., 1998. Kinetic Theory in the Earth Sciences. Princeton University Press.
Lear, C.H., Elderfield, H., Wilson, P.A., 2000. Cenozoic deep-sea temperatures and global ice volumes from Mg/Ca in benthic foraminiferal calcite. Science 287, 269–272.
Li, G., Elderfield, H., 2013. Evolution of carbon cycle over the past 100 million years. Geochim. Cosmochim. Acta 103, 11–25.
Misra, S., Froelich, P.N., 2012. Lithium isotope history of Cenozoic seawater: changes in silicate weathering and reverse weathering. Science 335, 818–823.
Mottl, M.J., Lawrence, J.R., Keigwin, L.D., 1983. Elemental and stable isotope composition of pore waters and carbonate sediments from deep sea drilling project sites 501/504 and 505. In: Initial Reports DSDP, vol. 69, pp. 461–473.
Mottl, M.J., Wheat, C.G., Monnin, C., Elderfield, H., 2000. Data report: trace elements and isotopes in pore water from Sites 1023 through 1032, Eastern Juan de Fuca ridge. In: Proc. ODP. In: Sci. Results, vol. 168, pp. 105–115. College Station, TX (Ocean Drilling Program).
Pagani, M., Caldeira, K., Berner, R., Beerling, D.J., 2009. The role of terrestrial plants in limiting atmospheric CO_2 decline over the past 24 million years. Nature 460, 85–88.
Pagani, M., Huber, M., Sageman, B., 2014. Greenhouse climates. In: Treatise on Geochemistry. 2nd edition, vol. 6, pp. 281–304.
Rahaman, W., Singh, S.K., Sinha, R., Tandon, S.K., 2011. Sr, C and O isotopes in carbonate nodules from the Ganga Plain: evidence for recent abrupt rise in dissolved $^{87}Sr/^{86}Sr$ ratios of the Ganga. Chem. Geol. 285, 184–193.
Rausch, S., Boehm, F., Bach, W., Kluegel, A., Eisenhauer, A., 2013. Calcium carbonate veins in ocean crust record a threefold increase of seawater Mg/Ca in the past 30 million years. Earth Planet. Sci. Lett. 362, 215–224.
Raymo, M.E., Ruddiman, W.F., 1992. Tectonic forcing of late Cenozoic climate. Nature 359, 117–122.
Richter, F.M., Rowley, D.B., DePaolo, D.J., 1992. Sr isotope evolution of seawater – the role of tectonics. Earth Planet. Sci. Lett. 109, 11–23.
Sen, I.S., Peucker-Ehrenbrink, B., 2012. Anthropogenic disturbance of element cycles at the Earth's surface. Environ. Sci. Technol. 46, 8601–8609.
Sleep, N.H., Zahnle, K., 2001. Carbon dioxide cycling and implications for climate on ancient Earth. J. Geophys. Res. 106, 1373–1399.
Spivack, A.J., Staudigel, H., 1994. Low-temperature alteration of the upper oceanic crust and the alkalinity budget of seawater. Chem. Geol. 115, 239–247.
Staudigel, H., 2014. Chemical fluxes from hydrothermal alteration of the oceanic crust. In: Treatise on Geochemistry. 2nd edition, vol. 4, pp. 583–606.
Staudigel, H., Muehlenbachs, K., Richardson, S.H., Hart, S.R., 1981. Agents of low temperature ocean crust alteration. Contrib. Mineral. Petrol. 77, 150–157.
Stein, C.A., Stein, S., 1994. Constraints on hydrothermal heat flux through the oceanic lithosphere from global heat flow. J. Geophys. Res. 99, 3081–3095.
Torres, M.A., West, A.J., Li, G., 2014. Sulphide oxidation and carbonate dissolution as a source of CO_2 over geological timescales. Nature 507, 346–349.
Vance, D., Teagle, D.A.H., Foster, G.L., 2009. Variable quaternary chemical weathering fluxes and imbalances in marine geochemical budgets. Nature 458, 493–496.
Veizer, J., Ala, D., Azmy, K., Bruckenschen, P., Buhl, D., Bruhn, F., Carden, G.A.F., Diener, A., Ebneth, S., Godderis, Y., Jasper, T., Korte, C., Pawellek, F., Podlaha, O.G., Strauss, H., 1999. $^{87}Sr/^{86}Sr$, $\delta^{13}C$ and $\delta^{18}O$ evolution of Phanerozoic seawater. Chem. Geol. 161, 59–88.
Walker, J.C.G., Hays, P.B., Kasting, J.F., 1981. A negative feedback mechanism for the long-term stabilization of Earths surface temperature. J. Geophys. Res., Atmos. 86, 9776–9782.
Wheat, C.G., Fisher, A.T., 2008. Massive, low-temperature hydrothermal flow from a basaltic outcrop on 23 Ma seafloor of the Cocos Plate: chemical constraints and implications. Geochem. Geophys. Geosyst. 9. http://dx.doi.org/10.1029/2008GC002136.
Wilson, D.S., Teagle, D.A.H., Acton, G.D., 2003. In: Proc. ODP. In: Init. Repts., vol. 206. College Station, TX (Ocean Drilling Program).
Zachos, J.C., Opdyke, B.N., Quinn, T.M., Jones, C.E., Halliday, A.N., 1999. Early Cenozoic glaciation, antarctic weathering, and seawater $^{87}Sr/^{86}Sr$: is there a link? Chem. Geol. 161, 165–180.
Zachos, J.C., Pagani, M., Sloan, L., Thomas, E., Billups, K., 2001. Trends, rhythms and aberrations in global climate 65 Ma to present. Science 292, 686–693.